Évaluation thermo-énergétique d'un stockage actif à matériaux à changement de phase intégrant une modélisation adimensionnée

Thermo–Energy Evaluation of an Active Phase Change Material Storage System Incorporating Dimensionless Modeling

Judith LUKAU M'NYAMPARA[1,2], **Ryad BOUZOUIDJA**[1,2*], **José Luiz LARA CRUZ**[3], **Cédric LE BOT**[1,2]

[1]University of Bordeaux, CNRS, Bordeaux INP, I2M, F-33400 Talence, France
[2] Arts et Métiers Institute of Technology, CNRS, Bordeaux INP, I2M, UMR 5295, F-33400 Talence, France
[3]Université de Pau et des Pays de l'Adour, LaTEP, Laboratoire de Thermique, Energétique et Procédés, 64000 Pau, France
*(Corresponding author: ryad.bouzouidja@u-bordeaux.fr)

Résumé - Cette étude analyse numériquement un système de stockage de chaleur latente à base de paraffine soumis à des cycles journaliers de charge–décharge, selon une approche adimensionnelle. Le changement de phase solide–liquide est modélisé à basse température en considérant les nombres de Biot, de Stefan et de Fourier ainsi que la température adimensionnelle θ. L'équation de la chaleur est résolue par volumes finis dans un code CFD interne, avec des conditions de type Robin dépendantes du temps. Les résultats montrent que θ constitue un paramètre clé pour l'optimisation des systèmes de stockage thermique à MCP.

Abstract - This study numerically investigates a paraffin-based latent heat storage system under daily charge–discharge cycles using a dimensionless framework. Solid–liquid phase change is modelled under low-temperature conditions, accounting for Biot, Stefan, and Fourier numbers and the dimensionless temperature θ. The heat equation is solved using an in-house finite–volume CFD code with time-dependent Robin boundary conditions. The results identify θ as a key parameter for optimizing PCM–based thermal energy storage systems.

Nomenclature (11 points, 2 colonnes)

a	thermal diffusivity, $\mathrm{m}^2.\mathrm{s}^{-1}$
c_p	specific heat capacity, $\mathrm{J.kg}^{-1}.\mathrm{K}^{-1}$
ΔH_m	Latent heat, $\mathrm{J.kg}^{-1}$
h	heat exchange coefficient, $\mathrm{W.m}^{-2}.\mathrm{K}^{-1}$
k	thermal conductivity, $\mathrm{W.m}^{-1}.\mathrm{K}^{-1}$
t	time, s
T	temperature, K
T_∞	external temperature, K
Bi	Biot number
Fo	Fourier number
Ste	Stefan number
f	volume fraction

Greek symbols

Φ	heat flux, W
ρ	density, $\mathrm{kg.m}^{-3}$
τ	characteristic time, s
θ	dimensionless temperature

Index and exponent

i	initial
m	melting
l	liquid
s	solid
ref	reference

https://doi.org/10.25855/SFT2026-115

1. Introduction

Improving the thermal performance of buildings is a major challenge in the context of the energy transition, as this sector accounts for a significant share of global energy consumption and associated greenhouse gas emissions [1]. Thermal energy storage systems, especially when coupled with renewable energy sources, constitute an effective strategy for reducing peak heating and cooling demands and attenuating indoor temperature fluctuations. In this context, phase change materials (PCMs) have attracted growing attention due to their high latent heat storage capacity over narrow temperature ranges, which makes them particularly suitable for low-temperature building applications [2].

PCM-based latent heat thermal energy storage has been widely studied for building applications, particularly for its potential to enhance thermal storage and energy efficiency. However, review studies have consistently highlighted key limitations related to heat transfer rates, phase change kinetics and properties (conductivity) and transient operation under realistic cyclic conditions [3], [4].

To address these limitations, among other things, a more fundamental analysis of the mechanisms governing heat transfer and their representation using dimensionless parameters is necessary.
From a heat transfer perspective, dimensionless analysis provides a powerful framework for interpreting phase change dynamics in latent heat storage systems. Several studies, including Le Bot et al. [5], have shown that dimensionless parameters such as the Biot number (*Bi*), the Stefan number (*Ste*), and the Fourier number (*Fo*) strongly condition the charging and discharging behaviour of PCM-based systems under cyclic thermal loading. Beyond these classical parameters, operating temperature amplitudes can be characterized through a dimensionless temperature parameter θ, comparing the imposed boundary temperature with respect to the PCM melting temperature. Ye et al. [6] demonstrated that this temperature difference can significantly affect energy release in PCM-based systems, particularly when it remains below 20 °C, while Le Bot et al. [5] fixed θ to focus on the influence of *Bi* and *Ste*. In this context, the present study addresses the role of θ as a control parameter for optimizing PCM-based thermal storage systems for building applications, by numerically modelling paraffin phase change using the in-house CFD code Notus under time-dependent thermal boundary conditions representative of daily charge–discharge cycles.

2. Modelling

2.1. Physical domain and boundary conditions

The physical domain and geometry considered in this study are identical to those used by Le Bot et al. [5] and are illustrated in figure 1 (a 2D rectangle of dimensions $15 \times 1\ cm$). Due to the small thickness of the domain, gravity effects are neglected, leading to a two-dimensional representation in which natural convection, radiation, and fluid motion are omitted, and heat conduction remains the dominant transfer mechanism. All boundaries are assumed adiabatic except the left boundary, where heat exchange with a heat transfer fluid (HTF) is modelled using a Robin (non-homogeneous Neumann) boundary condition. A constant heat transfer coefficient of $h = 200\ W \cdot m^{-2} \cdot K^{-1}$ is prescribed, allowing the HTF to either supply or extract heat from the PCM during the charge and discharge phases.

The fluid temperature, $T_\infty(t)$, varies periodically with time in order to represent the cyclic operation of the thermal storage system. Low values of T_∞ ($T_\infty < T_m$) correspond to the dis-

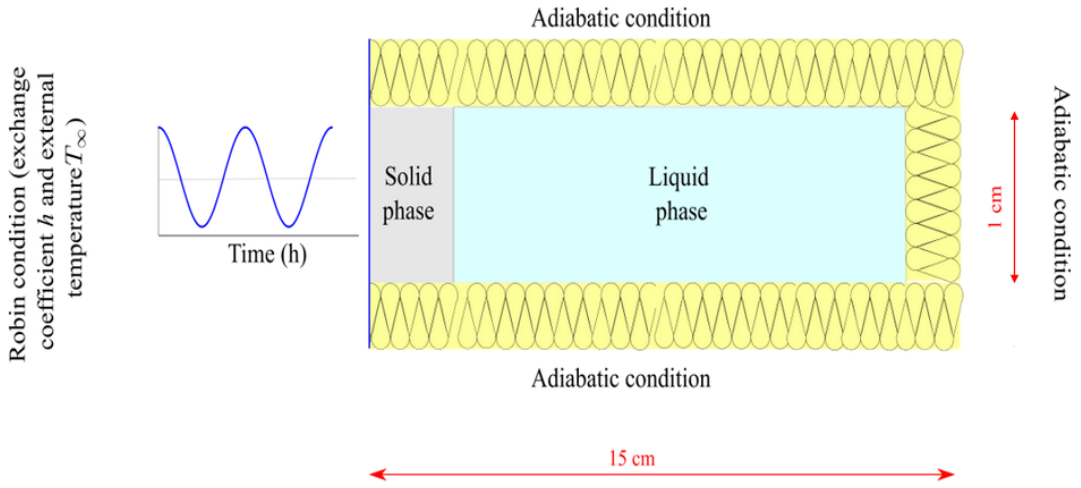

Figure 1 : *Numerical domain and PCM representation adapted from Le Bot et al. [5].*

charge phase, during which the PCM solidifies and releases heat to the heat transfer fluid (HTF), whereas high values ($T_\infty > T_m$) correspond to the charge phase, where the PCM melts while absorbing heat. The cycling process is characterized by the period τ, which governs the alternation between these two operating regimes. In the present study, $T_\infty(t)$ is prescribed as a sinusoidal signal of period τ, whose amplitude is controlled by the dimensionless temperature parameter θ, thereby enabling a systematic investigation of the influence of operating temperature amplitudes on the charge–discharge dynamics of the PCM.

The imposed external temperature (T_∞) is expressed in the following sinusoidal form (equation 1):

$$T_\infty(t) = T_m + \frac{T_{max} - T_{min}}{2} \cdot \sin\left(\frac{2\pi}{\tau}t + \frac{\pi}{2}\right) \tag{1}$$

The amplitude of the sinusoidal external temperature is selected so that the imposed temperature oscillates around the melting temperature of the phase change material. This amplitude is governed by the dimensionless temperature parameter θ, defined as the ratio between the difference of a reference temperature T_{ref} and the melting temperature T_m, and the difference between the initial PCM temperature T_i and T_m. The corresponding expression of θ is given in equation 2.

$$\theta = \frac{T_{ref} - T_m}{T_i - T_m} \tag{2}$$

Here, T_{ref} is defined as the mean value of the maximum and minimum imposed temperatures:

$$T_{ref} = T_m \pm \frac{T_{max} - T_{min}}{2} \tag{3}$$

The $\pm$ sign simply indicates whether T_{ref} is taken as T_{max} or T_{min} ; the physical amplitude remains positive.

Using the amplitude definition in terms of the parameter θ, the expression of $T_\infty(t)$ can be written as:

$$T_\infty(t) = T_m + (T_i - T_m)\theta \cdot \sin\left(\frac{2\pi a}{Fo\, L^2}\, t + \frac{\pi}{2}\right) \tag{4}$$

where the Fourier number *Fo* is defined as a function of the cycling period τ as given by equation 5. In the present study, the Fourier number is kept constant, together with the Stefan and Biot numbers (equation 6), through constant h, τ, T_i and physical properties in order to isolate the effect of the dimensionless temperature parameter θ.

$$Fo = \frac{a\,\tau}{L^2} \tag{5}$$

where a is the PCM thermal diffusivity and L the PCM length.

$$Bi = \frac{h\,L}{k} \qquad \text{and} \qquad Ste = \frac{c_p(T_m - T_i)}{\Delta H_m} \tag{6}$$

The phase change material considered in this study is the paraffin RT64HC, selected in continuity with works of Le Bot et al. [5] and Benbrika et al. [7]. In accordance with the thermal behaviour of paraffins, supercooling effects are neglected. Heat transfer within the PCM is described by the transient heat conduction equation under pure conduction assumptions. The thermophysical properties of the PCM are assumed constant and are reported in Table 1.

ρ	c_p	k	T_m	ΔH_m
kg.m^{-3}	J.kg^{-1}.K^{-1}	W.m^{-1}.K^{-1}	K	kJ.kg^{-1}
820	1900	0.2	337	230

Table 1 : *Thermophysical properties of the RT64HC paraffin [7].*

Initially, the physical domain is entirely filled with PCM in the solid state at a uniform temperature of $330\ K$ ($T_i < T_m$). Phase change occurs at the thermodynamic melting temperature T_m.

2.2. Governing equations

Heat transfer is described by the transient heat conduction equation (7), which governs the evolution of the temperature field within the PCM.

$$\rho c_p \frac{\partial T}{\partial t} = \nabla \cdot (k \nabla T) + S_c \tag{7}$$

Several numerical approaches have been proposed in the literature to model phase change. In the present work, phase change is modelled using a source term approach, recently implemented in the in-house CFD code Notus [9], based on a finite-volume discretization on a structured Cartesian grid. In this formulation, the latent heat effects are introduced through a source term S_c (equation 8), which represents the energy released or absorbed during phase change.

$$S_c = \rho L_f \frac{\partial f_s}{\partial t} \tag{8}$$

$$f_s = \begin{cases} 0 & \text{if } T > T_m, \\ 0 < f_s < 1 & \text{if } T = T_m, \\ 1 & \text{if } T < T_m. \end{cases} \tag{9}$$

The phase change process is solved using the iterative source term method originally proposed by Voller et al. [10]. This technique assumes that phase change occurs exclusively at the equilibrium melting temperature T_m, and the evolution of the solid fraction is determined accordingly (equation 9).
The algorithm is such that the source term ${S_c}^i$ is first initialized to 0, and the energy equation (7) is solved, giving the temperature field ${T_n}^{i+1}$. The source term is then updated from expression (10), where exponent i refers to the current internal iteration associated with the phase change algorithm, while the index n represents the time iteration.

$$ {S_c}^{i+1} = {S_c}^i + \frac{\rho c_p \left({T_n}^{i+1} - T_m \right)}{\Delta t} \tag{10} $$

Then, the source term ${S_c}^{i+1}$ is applied to expression (8) to estimate the solid fraction ${f_s}^{i+1}$. This updated source term ${S_c}^{i+1}$ is set in equation (7) to start a new internal iteration. The criterion: $\varepsilon = \sum \| f_{s,n}^{i+1} - f_{s,n}^{i} \| < 10^{-8}$ *or* 10^{-10} is checked until convergence.

3. Results and discussion

The simulations were performed using the in-house CFD code Notus over a sufficiently simulation long time to allow several successive charge and discharge cycles to develop, ensuring that a cyclic regime is established. A time step of $1\ s$ was used throughout the simulations. Since the numerical framework has already been validated against a semi-analytical Stefan–Neumann solution and experimental data in the work of Le Bot et al. [5], the present section focuses on the analysis of the charge and discharge behaviour of the phase change material through a parametric study based on the dimensionless temperature parameter θ.

The imposed Robin boundary condition generates a cyclic thermal response around the melting temperature T_m, whose amplitude is directly governed by the dimensionless temperature parameter θ. Figure 2 presents the temporal evolution of the boundary temperature at the convective interface for different values of the dimensionless temperature parameter $\theta = m \cdot \theta_{ref}$, with $\theta_{ref} = 0.714$, corresponding to the reference value adopted by Le Bot et al. [5]. As expected, the boundary temperature closely follows the imposed sinusoidal excitation, independently of the thermophysical properties of the phase change material.

The thermal response within the PCM is analysed through temperature profiles along the length of the PCM ($L = 0.15\ m$), at mid-height, shown in Figure 3. During the charging phase (t = $10.5\ h$), the temperature increase remains confined near the heated wall, while the core of the PCM stays close to the melting temperature. This behaviour indicates that a significant part of the supplied energy is absorbed as latent heat. During the discharging phase (t = $13.8\ h$), the temperature field becomes more uniform; however, for increasing values of the dimensionless temperature parameter θ, steeper thermal gradients persist within the material, preventing complete solidification within a single cycle.
These results illustrate the effective thermal buffering induced by latent heat effects within the PCM. In this range of operating conditions, the system behaviour is representative of realistic building applications, and the PCM efficiently attenuates temperature fluctuations inside the storage domain.

The heat flux exchanged at the left boundary is computed using Newton's relation $\Phi = h \cdot (T - T_\infty) \cdot S$, where h is the heat transfer coefficient, S the exchange surface, T_∞ the imposed external temperature, and T the boundary temperature obtained from the numerical model. The analysis focuses on a representative cycle selected once the cyclic regime is established, as illustrated by the second cycle in Figure 4. In this regime, the heat flux evolution on

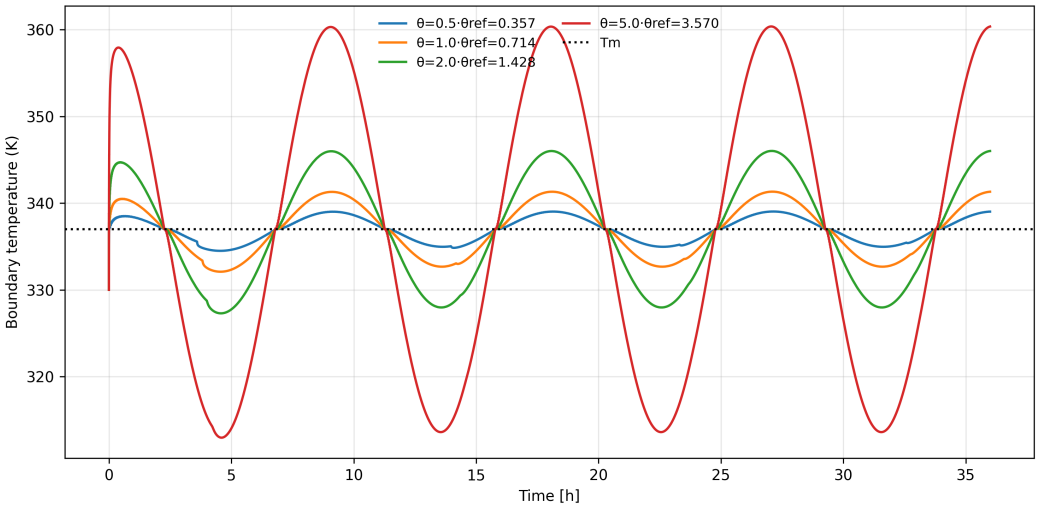

Figure 2 : *Boundary temperature evolution at the convective interface for different values of the dimensionless temperature parameter θ.*

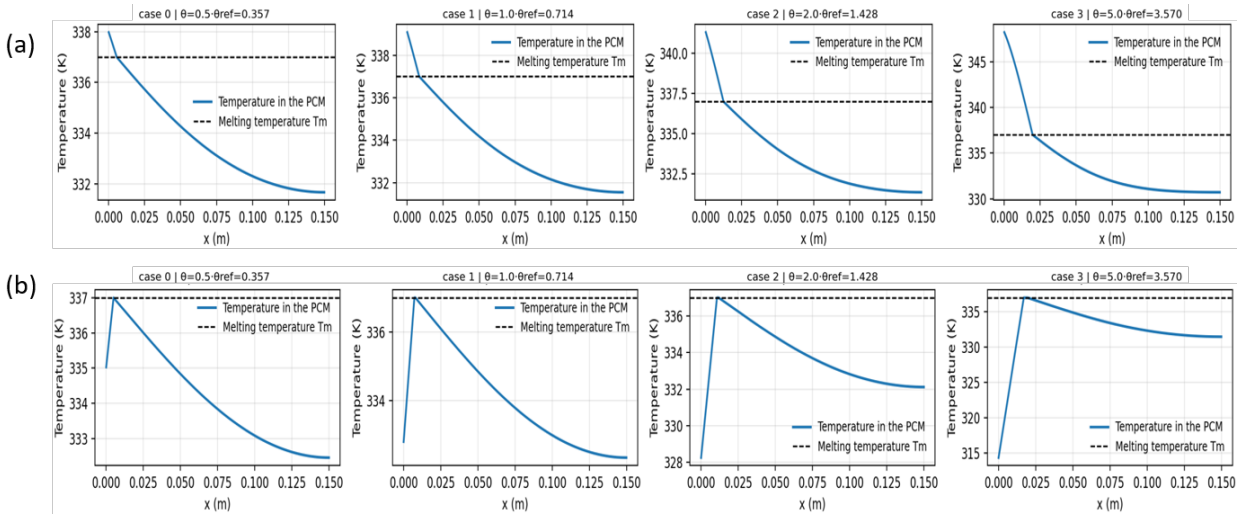

Figure 3 : *Temperature profiles along the length of the PCM during (a) charging (t = 10.5 h) and (b) discharging (t = 13.8 h) phases for different values of θ.*

the convective boundary clearly reflects the periodic thermal excitation and the influence of θ. Negative heat flux values correspond to charging phases, during which energy is absorbed by the PCM, whereas positive values indicate discharging phases associated with energy release. As θ increases, the amplitude of the heat flux increases in both phases, revealing stronger thermal solicitation and enhanced heat exchange at the boundary. Moreover, the temporal evolution of the flux differs between charging and discharging: for higher values of θ, this asymmetry is more pronounced because the flux exhibits steeper variations and longer relaxation times during discharge, associated with latent heat release and the progressive displacement of the solid–liquid interface. Conversely, for lower values of θ, the flux evolution becomes smoother and more regular, indicating operation closer to phase equilibrium and effective thermal buffering.

The phase change dynamics associated with these thermal conditions are illustrated in Figure 5, which shows the spatial distributions of the solid and liquid volume fractions at mid-height of the surface exposed to the heat flux during both charging (t = 10.5 h) and discharging (t = 13.8 h) phases. During cooling, a liquid layer is observed to remain temporarily trapped be-

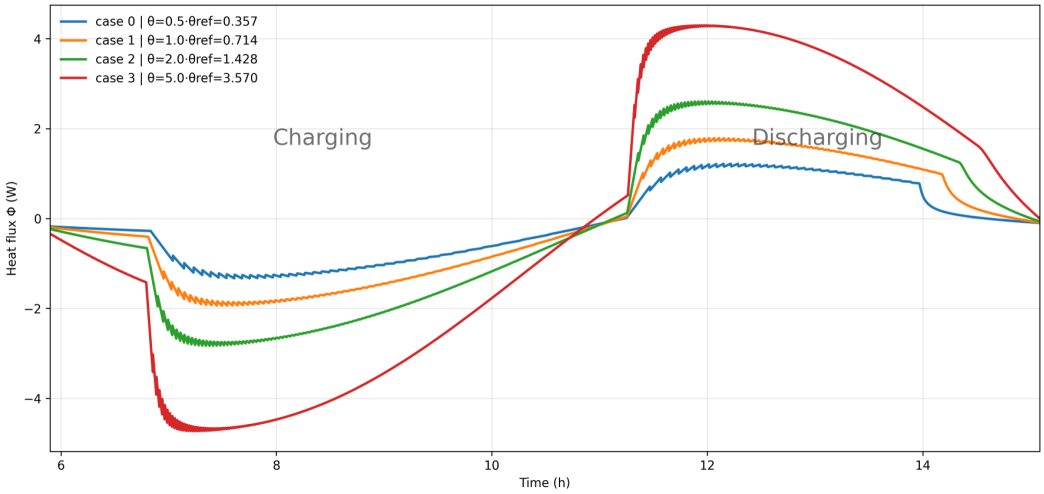

Figure 4 : *Time evolution of heat flux for different values of θ.*

tween two solid regions, indicating that the PCM does not fully solidify before the onset of the next thermal cycle. This behaviour is fully consistent with the temperature profiles discussed previously (Figure 3), which show persistent thermal gradients within the PCM for increasing values of the dimensionless temperature parameter θ. As a result, solidification may initiate simultaneously from different locations within the material, leading to transient liquid trapping. The thickness of this liquid layer increases with θ and becomes particularly pronounced for $\theta \geq 5.0\theta_{ref}$, confirming that solidification remains inherently partial under cyclic thermal excitation. These observations corroborate the thermal analysis and highlight the strong coupling between internal temperature fields and phase change kinetics under cyclic operating conditions.

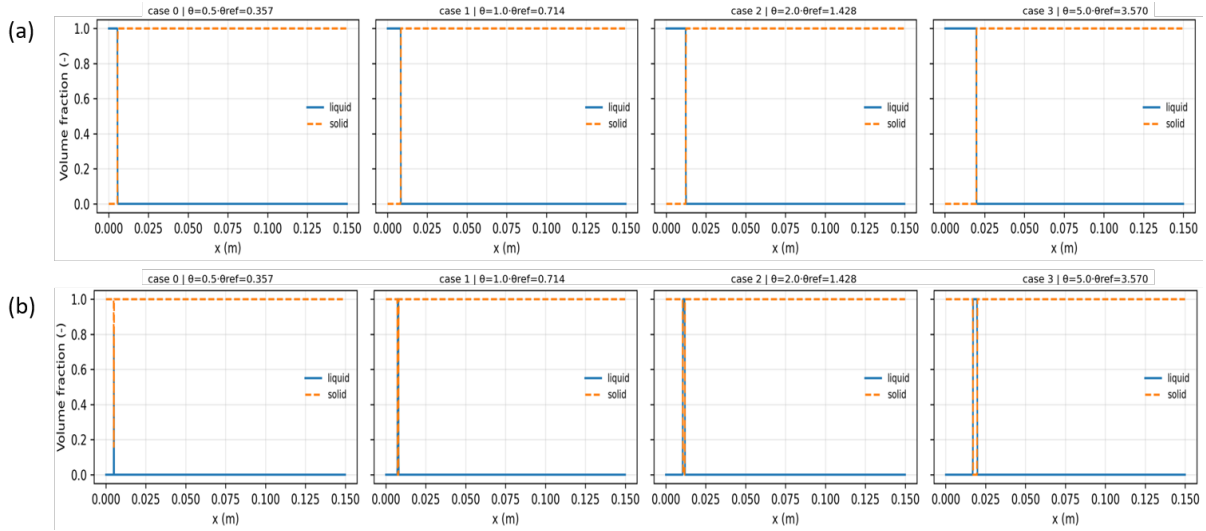

Figure 5 : *Spatial distributions of solid and liquid volume fractions during (a) charging (t = 10.5 h) and (b) discharging (t = 13.8 h) phases for different values of θ.*

4. Conclusion

This study investigated the thermo-energetic behaviour of a paraffin-based latent heat storage system under cyclic thermal excitation, with a particular focus on the dimensionless temperature parameter θ. The results show that low to moderate values of θ promote efficient thermal buffering, with internal temperatures remaining close to the melting point and regular

charge–discharge cycles representative of building applications. In contrast, higher values of θ lead to partial phase change, resulting in incomplete solidification and reduced latent heat utilization within a cycle. The heat flux analysis further highlights that both the amplitude and temporal evolution of heat exchange are strongly governed by θ once the cyclic regime is established, reflecting the kinetics of the phase change and the motion of the solid–liquid interface. Overall, θ is identified as a key parameter controlling the thermal performance of PCM-based systems. Future work will extend this study by incorporating convective effects, analyzing the full temporal evolution over complete cycles, and developing a fully dimensionless formulation, including the investigation of coupled effects between θ and the Fourier number.

References

[1] Global Alliance for Buildings and Construction (GlobalABC), *Global Status Report 2024: Towards a Zero-Emission, Efficient and Resilient Buildings and Construction Sector*, Report, 2025.

[2] K. Alassaad, J. Minto and P. de Wilde, Enhancing building thermal performance: A review of phase change material integration, *Energies*, 18 (2025) 3200.

[3] F. Agyenim, N. Hewitt, P. Eames and M. Smyth, A review of materials, heat transfer and phase change problem formulation for latent heat thermal energy storage systems, *Renewable and Sustainable Energy Reviews*, 14 (2010) 615–628.

[4] A. Sharma, V. V. Tyagi, C. R. Chen and D. Buddhi, Review on thermal energy storage with phase change materials and applications, *Renewable and Sustainable Energy Reviews*, 13 (2009) 318–345.

[5] C. Le Bot, A. Maftah, R. Bouzouidja and A. Sempey, Effect of Biot and Stefan numbers of a phase change material submitted to cyclic Robin conditions on the heat flux discharge, *International Journal of Thermal Sciences*, 205 (2024) 109280.

[6] W.-B. Ye, D.-S. Zhu and N. Wang, Numerical simulation on phase change thermal storage/release in a plate-fin unit, *Applied Thermal Engineering*, 31 (2011) 3871–3884.

[7] M. Benbrika, M. Benbelhout and M. Teggar, Amélioration de l'efficacité thermique d'un chauffe-eau solaire par l'utilisation de matériaux à changement de phase (MCP), *International Journal of Scientific Research & Engineering Technology (IJSET)*, Proc. 3^{e} Conférence Internationale des Énergies Renouvelables (CIER-2015), 2015.

[8] B. J. Kaaks, M. Rohde, J.-L. Kloosterman and D. Lathouwers, An energy-conservative DG-FEM approach for solid–liquid phase change, *Numerical Heat Transfer, Part B: Fundamentals*, 84 (5) (2023) 487–513.

[9] Notus CFD, *Notus CFD: Computational Fluid Dynamics software*, Software, Available at: `https://notus-cfd.org/`.

[10] V. R. Voller and C. Prakash, A fixed grid numerical modelling methodology for convection–diffusion mushy region phase change problems, *International Journal of Heat and Mass Transfer*, 30 (8) (1987) 1709–1719.

[11] S. P. Jesumathy, M. Udayakumar and S. Suresh, Heat transfer characteristics in latent heat storage system using paraffin wax, *Journal of Mechanical Science and Technology*, 26 (3) (2012) 959–965.

Acknowledgements

The authors gratefully acknowledge the financial support for the doctoral study of Judith Lukau M'Nyampara provided by the University of Bordeaux. The authors would like to thank the Region Nouvelle Aquitaine related to Project PSGAR-session 2 Energie CERENA 38891920-38899520. Finally, the authors would like to thank the Carnot ISIFoR institute for its support and funding.